Archaeological and Anthropological Sciences (2021) 13:79
https://doi.org/10.1007/s12520-021-01309-0

ORIGINAL PAPER

From ancient construction, through survival, towards modern conservation: characterization of fine-grained building material at Niğde-Kınık Höyük (Cappadocia, Turkey)

Massimo Setti[1] · Anna Arizzi[2] · Paula Nieto[3] · Nicolás Velilla Sánchez[2] · Giuseppe Cultrone[2] · Lorenzo d'Alfonso[4,5]

Received: 18 December 2020 / Accepted: 28 February 2021

Abstract

In this paper, we studied building materials from the Niğde-Kınık Höyük archaeological site (Southern Cappadocia, Turkey) with the support of historical, architectural, and geological research. The samples were collected within the framework of the *Kınık Höyük Archaeological Project*, which began excavations at the site in 2011 in a bid to conserve the ancient buildings that would be discovered there. The objective was to characterize the fine-grained building materials as a means of understanding the structural stability they offered, in order to explain how the remains had managed to survive for such a long time. Samples were taken from the coating on different walls, from mud bricks and rendering, and from soil-beaten floors from the different buildings in the settlement. Samples were first observed using a video microscope and then studied by means X-ray diffraction and optical and scanning electron and transmission microscopies. The materials studied were composed of volcanic sands coming from the materials that outcrop in the area. In general, the samples were porous and fissured and minerals of volcanic origin were identified such as quartz, plagioclases, cristobalite, pyroxenes, micas, amphiboles, and olivine together with others of sedimentary origin, such as calcite, and small amounts of clays. The possible presence of hydrated calcium silicates was closely investigated due to their important role in the preservation of ancient building materials, but although we searched for them with a range of different techniques, none was found. This indicates that the long-term conservation of the Niğde-Kınık Höyük archaeological site may be due to the fact that it was buried at constant temperature and humidity conditions and so protected from the weather conditions, which are milder in this area than in any other region of Central Anatolia.

Keywords Niğde-Kınık Höyük · Earthen material · Mineralogy · Petrography · Volcanic sands · Clay

Introduction and objectives

The oval-shaped mound of Niğde-Kınık Höyük[1] (Fig. 1) lies about 1 km from Bayat, a village in the northern part of the Bor plain, to the west of the town of Niğde and at the foot of the Melendiz volcanic complex in southern Cappadocia (Turkey).

The archaeological site of Niğde-Kınık Höyük covers about 24 ha and contains various structures, including an acropolis, a terrace, and a lower city. A geophysical survey was conducted in 2010 combining magnetometry and GPR (ground-penetrating radar). The survey could identify the citadel walls in a good state of conservation that were 4–5 m

[1] DMS geographical coordinates of the geodesic point on the mound: N 37° 56′ 14.3988″, E 34° 22′ 48.7308″ (source: Google Earth, verified by GPS)

✉ Anna Arizzi
arizzina@ugr.es

[1] Department of Earth and Environmental Sciences, University of Pavia, via Ferrata 1 - 27100, Pavia, Italy

[2] Department of Mineralogy and Petrology, Faculty of Sciences, University of Granada, Avda. Fuentenueva s/n, 18002 Granada, Spain

[3] Department of the Environment, CIEMAT, Avda. Complutense 22, 28040 Madrid, Spain

[4] Institute for the Study of the Ancient World, New York University (ISAW-NYU), 15, East 84th St, New York, NY 10028, USA

[5] Department of Humanities, University of Pavia, P.za del Lino 2 - 27100, Pavia, Italy

Published online: 09 April 2021

Fig. 1 Niğde-Kınık Höyük archaeological site (Turkey). Kınık Höyük Archaeological Project. Image from: https://www.kinikhoyuk.org

thick and showed a preserved height of 12–15 m, including foundations (d'Alfonso 2010; d'Alfonso and Mora 2012; Balatti and Balza 2012). The results of magnetometry and GPR data also hinted at the presence of a second fortification wall around the edge of the terrace (d'Alfonso et al. 2014).

This region is very important from a historical, archaeological, and geological perspective. In fact, the site seems to have been chosen as a suitable place for a settlement due to a combination of factors that would have allowed a population to sustain itself and develop there: the abundance of raw materials (such as gold, silver, tin, iron, obsidian, alabaster, and marble), the availability of water (Balatti and Balza 2012), and its strategic position between some of the main communication routes from prehistoric times right through to the Medieval era (Matessi et al. 2014). All of these factors enabled Niğde-Kınık Höyük to be inhabited for around 4,000 years (Cinieri et al. 2014).

In spite of its historic importance, the first intensive survey at Niğde-Kınık Höyük did not begin until 2006 (d'Alfonso and Mora 2007) and the excavations commenced 5 years later (Cinieri et al. 2014). Together with the archaeological excavations, after the results of the geophysical survey, the aim was also to conserve the main architectural structures and to promote the idea of the archaeological site being turned into a museum in the future (Cinieri et al. 2016).

In geological terms, this area is characterized by the important volcanic activity that took place during the Quaternary and the Neogene and the presence of alluvial and lacustrine deposits, which indicate that the Bor Plain was covered by a lake during the Pleistocene (Altın et al. 2015).

Niğde-Kınık Höyük is located in a plain at the foot of various volcanoes and the area is therefore characterized by volcanic rocks (dacitic to rhyolitic ignimbrite) (Dhont et al. 1998; Deniel et al. 1998; Innocenti et al. 1975, 1982a, 1982b; Pasquaré et al. 1988; Kurkcuoglu et al. 1988; Kuşcu and Geneli 2010; Piper et al. 2013; Toprak 1994). It is therefore not surprising that the stones used in the masonry are mainly basalt and andesite. We decided to start investigating the composition of the earthen materials (surface finishes, renders, mortars, mud bricks, and loose materials) in order to study their properties, thus contributing to a finer understanding of the construction techniques used by the ancient builders and to try to ascertain how these may have influenced the long-term stability and durability of architectural remains at the site.

With this in mind, we approached the earthen building materials in the context of the local construction techniques as well as the local geology, so as to acquire a more detailed knowledge of the region. We then carried out a chemical-mineralogical, petrographic, and textural study of samples from the archaeological site so as to determine their composition and manufacturing process. One specific objective was to investigate whether the building materials used in the wall were hydraulic, which could explain their high durability and preservation over several thousand years. In particular, we aimed to discover whether the conditions were favorable for the formation of calcium silicate hydrates (CSH), which are known to be produced by the hydration of both natural (Cerny et al. 2006) and artificial (Theodoridou et al. 2013) hydraulic binders and/or admixtures. These compounds could have been formed from the reactant silica compounds present in the earth used in the building materials, after reaction with calcium oxide or hydroxide in the presence of moisture (Cizer 2009). Given this

possibility, we decided to investigate the possible use of lime in the manufacture of these materials.

Finding out more information about the construction technology used in the wall is also essential for planning suitable restoration and/or conservation strategies for the Niğde-Kınık Höyük archaeological site.

Archaeological and construction analysis

In 2011, an archaeological project organized jointly by Pavia University (Italy) and the Institute for the Study of the Ancient World (ISAW, New York University, USA) started excavations at Niğde-Kınık Höyük in Southern Cappadocia. The site was chosen after 4 years of archaeological surveys along the southern side of the Melendiz Mountains. Surface materials collected in the intensive survey program at the site suggested that it had been occupied at different times in the Late Bronze Age (LBA), Early Iron Age (EIA), and Middle Iron Age (MIA) (d'Alfonso and Mora 2010; d'Alfonso et al. 2014 and 2020). Excavations during the last 10 years have confirmed that the site offers a unique example of continuity of political complexity in the transition from the Bronze towards the Iron Age, at the turn of the second millennium BC. However, excavations have also shown the presence of continuity of occupation and Anatolian cultic practice and architectural technique from Iron Ages down to the Hellenistic period (d'Alfonso and Castellano 2018; d'Alfonso et al. 2020). The following site periodization has been thus defined:

KH-P I = ca 1100–1400 AD
KH-P II = ca. 150–30 BC
KH-P IIIA = ca. 350–150 BC
KH-P IIIB = ca. 550–350 BC
KH-P IV - ca. 800–600 BC
KH-P VA = ca. 1050–800 BC
KH-P VB = ca. 1200–1050 BC
KH-P VI = ca. 1600–1200 BC

While LBA and Hellenistic architecture of Anatolia have been widely studied, we concentrated our investigations on the Iron Age earthen building materials and their relevance for reconstructing the building technique of this period in Central Anatolia. Besides timber, in all ages, the construction materials come from the surrounding area and are therefore of volcanic origin. In particular, the masonry stones are composed of andesite and basalt and the mud used in the renders and mud bricks was manufactured out of volcanic sediments that were rich in glass and other minerals (Gürel and Lermi 2010).

As regards the very good state of conservation of the Niğde-Kınık Höyük archaeological area, particularly its earthen components, this is indeed remarkable. It does not depend on extensive fires which backed bricks and renders, as is the case in several other sites (e.g., Özgüç 2005; Beyer 2010 and 2015; Highcock et al. 2015; Larsen 2015). As all *hoyuks*, architectural remains have been covered by sediments and they have spent a long time buried at constant temperature and humidity conditions. Moreover, this area has a semi-arid to continental climate, with average annual precipitations of 325–350 mm: this is by far less impactful than average precipitations in any other region of Central Anatolia. Nonetheless, the wide variation in the annual average temperature from 0 °C in January to 23 °C in July (d'Alfonso et al. 2014; MGM 2019) and the strong winds caused a decline of the exposed architecture, only mitigated by the sheltering.

Materials and methods

During the archaeological excavations in 2013 and 2014, 50 samples of different types of building components from the different periods to the Iron Ages were collected and shipped to our laboratories in the frame of a collaboration with Dr. Ai Gurel, from the Niğde University. In this paper, we present the results for 14 representative samples taken from the following types of building (Table 1 and Fig. 2): the plaster/render of the EIA fortification wall (KH-P VA); the outer surface of the MIA defensive ramp (KH-P IV), from Sector Aw (operation A, Fig. 3); mud brick, beaten earth floor, render, and white-colored film from Late Iron Age (LIA) rooms Ar1 and Ar15 (KH-P IV), in Sector A2 (operation A, Fig. 3); mud bricks, render, and outer film from the Yellow Building (Achaemenid Period, KH-P IIIB) in Sector B2, on the southern summit of the mound (operation B, Fig. 3). We also took two samples of sandy sediments from the soil on the mound to compare their composition with that of the archaeological samples.

An initial general observation of the samples was made using a Leica VDM 2000 video microscope with Leica Application Suite V.3.8.0. software. For the petrographic characterization of the samples, six polished thin sections were prepared from renders, mortars, and mud bricks (A1, A11b, A14, A17, B6, and B8; Fig. 2). The samples were very fragile and were coated with resin to protect them. They were then observed with a Carl Zeiss Jenapol-U polarized optical microscope (POM) equipped with a Nikon D7000 digital camera, with the aim to identify the mineral phases, describe the microstructure of samples (i.e., grains size, porosity, etc.), and investigate the presence of pathologies.

Mineralogical analyses were carried out by X-ray diffraction (XRD) on powder from the bulk sample, using a Philips PW 1800 diffractometer with CuKα radiation (45 kV, 35 mA), 2° to 65° 2θ, and a scan speed of 1° 2θ/min, software processing X'Pert High Score v.4.6a. A second diffractometer was also used, a PANalytical X'Pert Pro (detector X'Celerator), with the following working conditions: CuKα radiation, 45 kV, 35 mA, 4° to 70° 2θ explored area and 1° 2θ/

Table 1 Description of samples from Niğde-Kınık Höyük archaeological site: name, building typology, and location in the site

Sample name	Building typology	Location in the site
A1	Mud rendering	SU A11 of the EIA citadel walls
A10	Earthen surface	SU 1820 of the MIA defensive ramp attached to the city wall
A11b	Mud brick with mud rendering and white surface finish	Wall A300, room Ar1, LIA
A14	Mud brick	Wall A234, room Ar1, LIA
A17	Mud brick	Wall A234, room Ar1, LIA
A18	Mortar fragment attached to the floor	A1245, room Ar1, LIA
A20	Cinder layer with pumice stone fragments	Wall 10 cm thick, Room Ar1, LIA
A23	Rendering mortar made with raw mud	Wall A1244, room Ar1, LIA
A27	Rendering mortar made with raw mud	Wall A234, room Ar15, LIA
A27b	White surface film on mud render	Wall A234, room Ar15, LIA
A29	Mud brick	Wall A234, room Ar15, LIA
A32	Mortar floor	SU A280, room Ar15, LIA
B1	Rendering mortar made with raw mud	Wall B897, room Br7, KH-P IIIB
B6	Rendering mortar	Wall B673, room Br7, KH-P IIIB
B8	Mud brick	Wall B397, room Br7, KH-P IIIB

min goniometer speed. Some of the samples were sieved in order to determine the variability of the mineralogy in terms of grain size. The fractions were divided into three groups: from 1 to 0.2 mm, from 0.2 to 63 μm, and less than 63 μm, in order to identify the mineral phases composing each fraction.

The microstructural characterization of the samples and the chemical composition of selected points or areas were studied using two high-resolution scanning electron microscopes. One was a Zeiss SUPRA40VP variable pressure scanning electron microscope (VPSEM) and the other was a Carl Zeiss SMT field emission scanning electron microscope with a focused ion beam (FIB-FESEM) (AURIGA Series), both coupled with EDX microanalysis. Five polished thin sections previously observed under POM (A1, A11b, A14, A17, and B8) and four

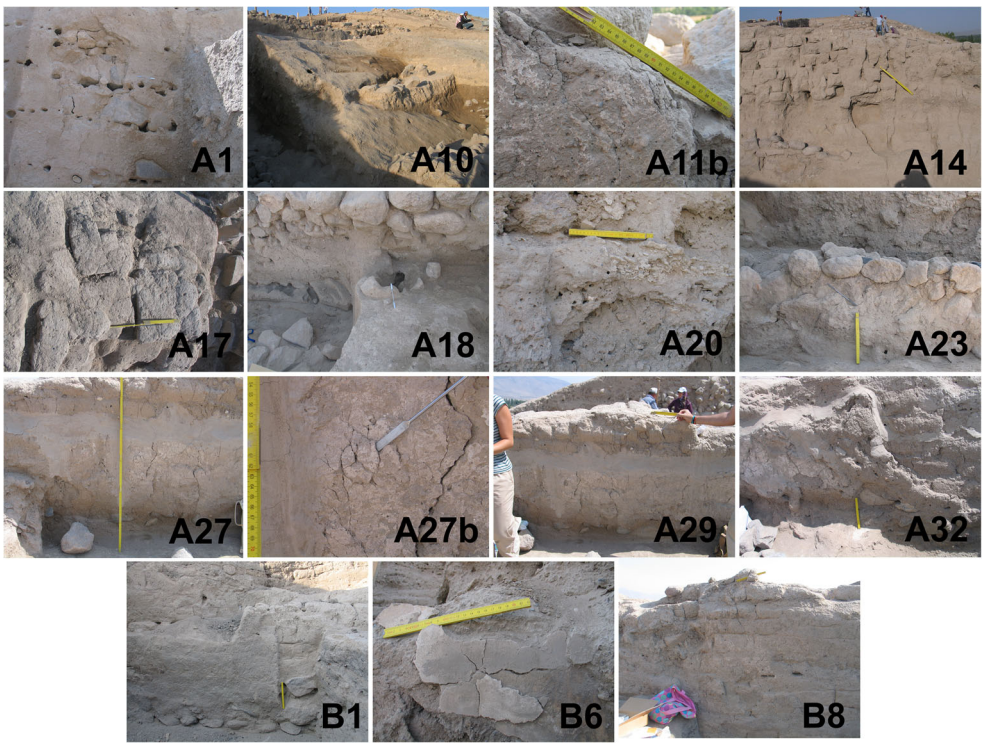

Fig. 2 Photographs of the areas of Niğde-Kınık Höyük where samples were collected

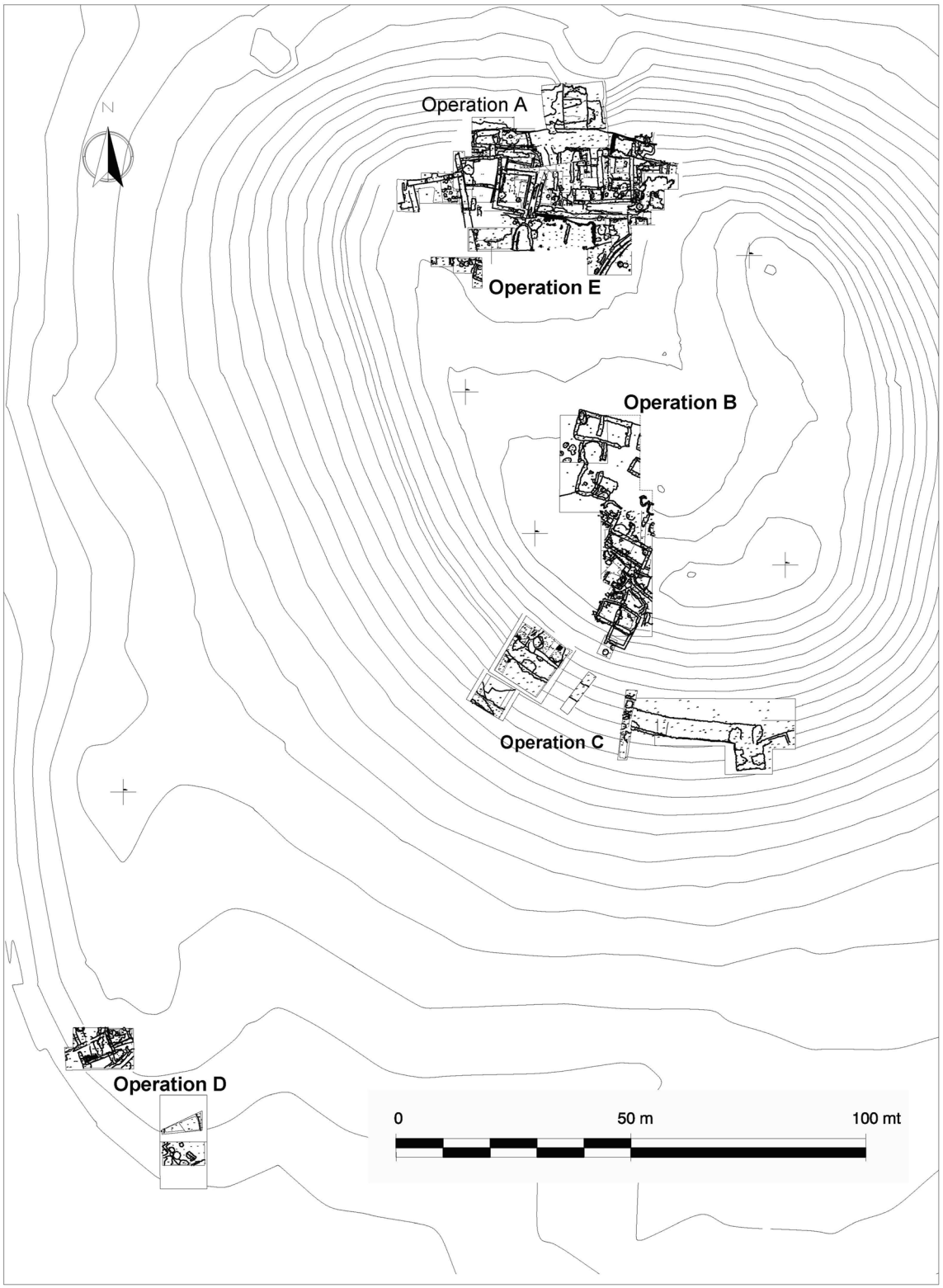

Fig. 3 2020 topographic plan of Map of Niğde-Kınık Höyük with excavated trenches (survey L. Davighi)

small carbon-coated fragments (A1, A10, A14, B8) were observed by VPSEM and FIB-FESEM, respectively.

Two samples (a mud brick, A14, and a rendering mortar, B6) were studied using a Titan high-resolution scanning electron microscope (HRTEM) with an XFEG emission gun, a spherical aberration corrector, and an HAADF detector, operating at 300 kV accelerating voltage. The resolution of this apparatus is 0.8 Å in the HRTEM mode and 2 Å in the scanning

transmission electron microscopy (STEM) mode. Quantitative chemical analyses in STEM mode were performed using the Titan's Super-X detector. Mineral standards were used to obtain the K-factors according to the method proposed by Lorimer and Cliff (1976). The powder samples were deposited on carbon-coated Cu grids. The aim of this technique was to search for possible amorphous/nanocrystalline phases of hydraulic phases such as calcium silicate hydrates (CSH), the presence of which could have contributed to the good state of conservation of the Niğde-Kınık Höyük archaeological site.

Finally, the study of the porous system of four archaeological samples with different building typology (A14, A27, A32, and B6) was performed with mercury intrusion porosimetry (MIP) using a Micromeritics AutoPore IV 9500 porosimeter. The pore size distribution was analyzed within a range of between 0.002 and 200 μm. Samples of about 1 cm^3 were oven-dried at 70 ± 5 °C for 8 h before being analyzed. The specific surface area (SSA), open porosity (P_o), and apparent and real densities (ρ_a and ρ_r) were also calculated.

Results and discussion

Video microscope observation

In general, all the samples had a similar appearance: they were composed above all of volcanic sands with a fine grain size with some grains of up to 2 or 3 mm which could be seen with the naked eye (Fig. 4). These grains were relatively compact, but could be manually broken down into smaller fragments or crumbs without applying much pressure. The general color was beige/greyish and the biggest grains varied in shade from the dark colors typical of volcanic glass or melanocratic minerals such as pyroxenes, amphiboles, or black micas, to the lighter colors typical of quartz and feldspars. There were also frequent yellowish areas which may have been related with the presence of oxides/hydroxides. Most of the samples had numerous pores and fissures. In those that had relatively few pores, the grains appeared to have better cohesion (sample A20) and they were more resistant to manual crumbling. A fine white surface layer was observed on the samples from exterior renders (A11b, A27b, A32, B6; Fig. 4). In a fragment of paving (sample A32), three layers of different colors were clearly discernable—the top layer was white, the middle layer was beige-brown, and the third layer was a lighter beige (Fig. 4). Sample A18 stands out for its white color, very fine grain size, and small fissures (Fig. 4).

X-ray diffraction

As can be seen in Table 2, no substantial differences were observed between the mineralogy of the local terrain and that of the materials used in the constructions at the Niğde-Kınık Höyük settlement. Mineralogical analysis showed that the mortars and mud bricks had a relatively homogeneous mineralogical composition and were free of clay minerals. In order of abundance, the main mineral constituents were cristobalite, tridymite, quartz, feldspars

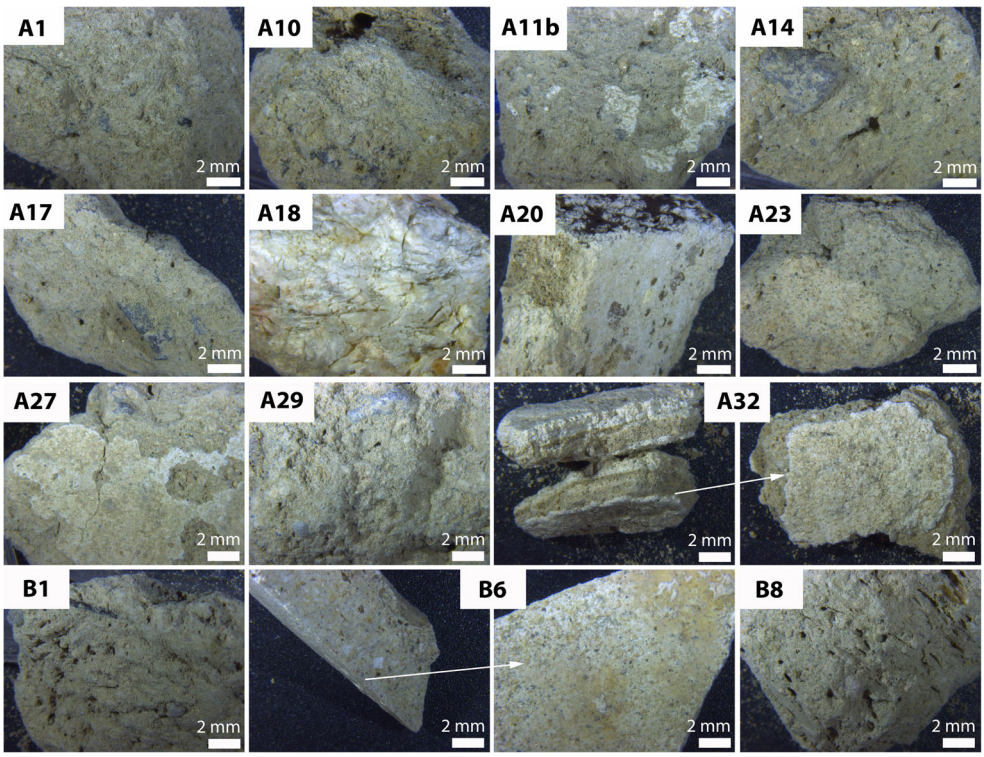

Fig. 4 Photographs of the samples taken under the video microscope

Table 2 Mineralogical composition of the samples studied using XRD

Sample	Majority phases	Minority phases
A1	Calcite, plagioclase, quartz	Cristobalite, gypsum, halite, pyroxene
A10	Calcite, plagioclase, quartz	Amphibole, cristobalite, mica
A11b	Cristobalite, plagioclase, quartz	Calcite, pyroxene, mica
A14	Calcite, plagioclase, quartz, cristobalite	Tridymite, pyroxene, mica
A17	Cristobalite, plagioclase, quartz	Calcite, mica
A18	Quartz	-
A20	Cristobalite, plagioclase, sanidine	Calcite, quartz
A23	Calcite, plagioclase, quartz, cristobalite	Pyroxene, mica
A27	Cristobalite, plagioclase, quartz	Calcite, mica
A27b	Calcite, plagioclase, quartz	Cristobalite, mica
A29	Cristobalite, plagioclase, quartz	Calcite, mica
A32	Plagioclase, quartz	Calcite, mica, cristobalite
A32	Calcite	-
B1	Cristobalite, plagioclase, quartz	Calcite, mica
B6	Calcite	Plagioclase, quartz
B8	Cristobalite, plagioclase, quartz	Calcite, mica
T1	Cristobalite, plagioclase, quartz	Calcite, mica
T4	Cristobalite, plagioclase, quartz, calcite	Mica

s.l., and calcite ($CaCO_3$). Mica and amphibole were sometimes present, albeit in small quantities, while gypsum ($CaSO_4 \cdot 2H_2O$) and halite (NaCl) were identified in only one sample (A1). Cristobalite and tridymite are two polymorphs of silica (SiO_2) which originated from volcanic glass following hydrothermal phenomena. The profile of the peak around 22° 2θ was identified as cristobalite/tridymite, but according to the classification proposed by Smith (1998), it could also perhaps belong to Opal-C. It therefore cannot be ruled out that certain forms of non-crystalline opal (Opal-A) and perhaps of volcanic glass may also be present. In the soil samples from the rampart, the peak at 22° 2θ is broader and could be attributed to Opal-CT.

The presence of calcite in the soil indicates that lime was not necessarily added to the raw material used in the construction. Larger amounts of calcite can be observed in the finest soil fraction (T4), which could possibly indicate that it is part of the microcrystalline fraction of the samples. Larger amounts of calcite were also observed in the white surface finishes of the renders (A27b and A32) than in the samples as a whole. This would suggest that the surface finishes were indeed made with lime. We also analyzed a white grain found in the hardest mortar (B6), which turned out to be tridymite.

It is important to remember that although under the video microscope we identified volcanic glass as one of the components of the samples, this was not detected by XRD, as this technique is unable to identify amorphous phases.

Polarized optical microscopy

Under polarized optical microscope observation, the samples had a similar appearance. Pores and fissures were quite abundant, with the exception of sample B6, which was much more compact. The matrix of the samples had a fine grain size and was light brown in color with yellowish or ochre brown areas denoting the presence of Fe oxides/hydroxides (Fig. 5). This matrix constituted over 80% of the sample and contained abundant amounts of ignimbritic material, attributable to volcanic glass, a phase that could not be detected by XRD. The size of the grains in the matrix made most of them optically indistinguishable, although some small calcite crystals could be identified. Dental fragments were found in one of the samples (as was later confirmed by EDX analysis during the observation of the samples under SEM).

The matrix contains both monomineralic grains and fragments of rock, although the former predominate. The size of these grains varies, although the most common grain size is between 0.15 and 0.4 mm. The morphology is also variable, ranging from angular to rounded grains, which in general would suggest a short-to-medium transport of the materials. The grains correspond above all to feldspars (plagioclases), followed by quartz, with very small amounts of mica, amphibole, pyroxene (Figs. 5a and b), and olivine crystals. This last phase in particular could not be detected by XRD because the amounts were below the limit detectable by the X-ray diffractometer. Crystals of metallic ores and of oxides/hydroxides appear throughout the sample, both scattered and in clusters.

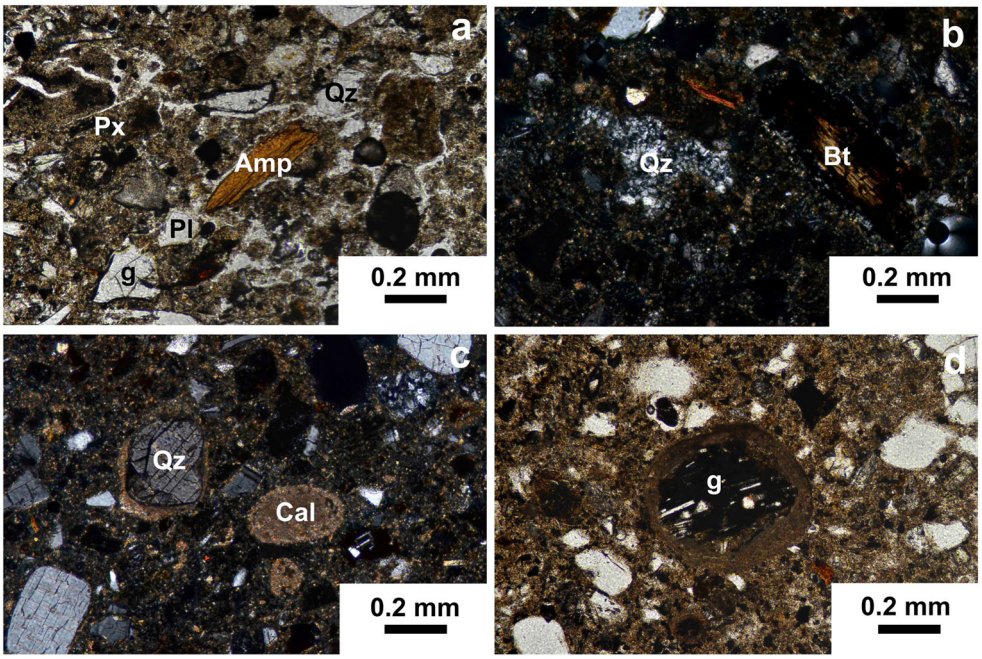

Fig. 5 Optical microscopy images of **a** sample B1 where quartz (Qz), plagioclase (Pl), pyroxene (Px), and amphibole (Amp) crystals and fragments of volcanic glass can be seen within a yellowish-brown matrix (plane light). **b** Sample A1 in which a biotite crystal (Bt) with an aureole of Fe oxides stands out and, to its left, a microcrystalline quartz (Qz) (cross polars). **c** Sample B8 showing a very fine-grained rim around a quartz grain (Qz) and, to its right, a grain of calcitic micrite (Cal) with the same composition as the rim (cross polars). **d** Sample A11b in which a fragment of volcanic glass (g) that contains thin plagioclase crystals is surrounded by a similar rim to that observed in **c** (plane light)

The rock fragments have quite variable morphologies and textures with both angular and rounded shapes and grain sizes varying from between just a few tens of micrometer to several millimeter (Figs. 5a and d). These fragments vary in nature and could be attributed to volcanic glass or to different kinds of volcanic rocks ranging from basic (mainly basalts) to intermediate (andesites) and acidic compositions (rhyolites). Fragments of glass are very common. These are transparent or grey in color under plane polarized light and are easy to identify because they show complete extinction when the nicols are crossed due to their amorphous nature.

Also worth noting is the presence of very fine brown rims around some of the fragments of volcanic rock and silicate grains. These rims were also observed around quartz crystals and micritic calcite clusters (Figs. 5c and d).

Scanning electron microscopy and compositional analysis

Using EDX analyses, we were able to identify or confirm the nature of some of the rocks and the dark rims observed under POM around the silicates and rock fragments. We also analyzed fragments of volcanic glass, obtaining in general silica-rich compositions with varying amounts of Fe, Mg, Na, Al, Ca, and K.

Compositional maps of the elements were obtained in some of the grains of special interest in order to obtain detailed information about their chemical composition. Figure 6 shows a more magnified image of the same fragment of volcanic rock observed earlier using POM (Fig. 5d) and composed above all of glass and plagioclase crystals. The distribution of elements indicates that the dark color observed in the thin section is due to a concentration of Fe and Ti oxides/hydroxides. The rim around it is mainly composed of Ca and probably corresponds to a microcrystalline aggregate of calcite.

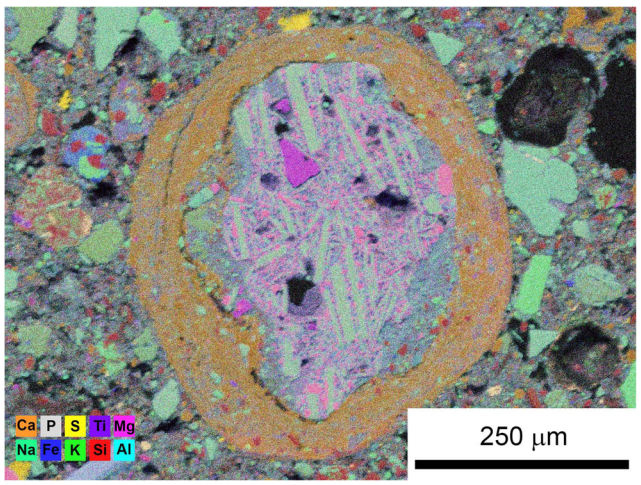

Fig. 6 Compositional map of the elements (sample A11b) in a fragment of volcanic rock rich in glass and plagioclase crystals around which a white aureole rich in Ca has developed

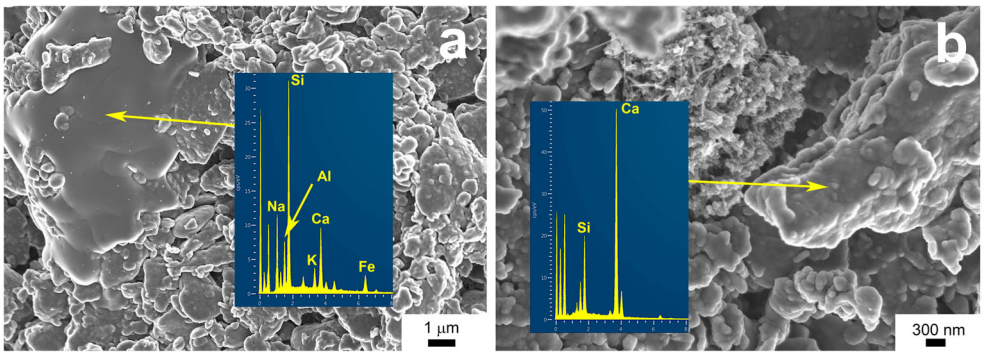

Fig. 7 SEM images obtained using secondary electrons with their corresponding spectra. **a** Particles that make up sample A1 and the film covering them. **b** Particles that make up sample A14 with compositions very rich in Ca and silica

The observation and EDX analysis of fragments of samples under SEM enabled us to identify certain phases, such as gypsum or halite, which also appear in the XRD analyses, though they were not found during POM observations (as they had possibly leached off by water during preparation of the thin sections). We also studied the composition of a film covering the grains that prevented us from fully distinguishing their morphology. In fact, as can be seen in Fig. 7a, the particles beneath the film are themselves formed by other smaller particles, which together form a relatively porous structure. The EDX analyses show that both the particles and the film covering them have siliceous compositions with abundant amounts of calcite.

It is possible that compositions as rich in Ca as that observed in Fig. 7b are due, firstly, to the abundant presence of the microcrystalline calcite that forms the matrix and, secondly, to the fact that the siliceous compositions come from minerals or glass of volcanic origin. We studied the intensity relationships of the spectral lines of different elements of the EDX spectra in order to find out whether any hydrated calcium silicate phases (CSH) were present. However, none of the analyses carried out was compatible with the intensity relationships corresponding to these phases.

With SEM, we also identified a range of crystals commonly found in volcanic rocks, which had also been observed with other techniques. These included quartz, plagioclase, pyroxenes, and micas as well as the odd olivine crystal, possibly produced by the basaltic volcanism present in the area.

Transmission electron microscopy, electron diffraction, and compositional analysis

Unlike the other techniques, TEM was used to identify the minerals in the clay. This was because these minerals were only present in the finest fraction (the part analyzed by TEM) and in such low quantities as to make it impossible for them to be identified by XRD analysis of the whole sample. Sample A14 has a higher clay content than sample B6, which has a higher carbonate content.

As regards the clayey minerals, smectite particles were observed forming aggregates of tiny laminar crystals (Fig. 8). The compositions of these crystals were determined using AEM. On the basis of the intensities recorded in the spectra for the elements of which they are composed, we arrived at their structural formulas (Table 3). This information was then used to classify them. The three smectites analyzed turned out to be montmorillonites. Figure 8a shows the smectite corresponding to sample B6 and Fig. 8b the one corresponding to sample A14(2). Other clayey minerals detected included kaolinite (Fig. 8b) and illite, although these appeared in smaller amounts in the preparation made for TEM.

In addition to the phyllosilicates, we also observed particles with a different, essentially granular morpholo-

Table 3 Structural formulas for smectites (based on $O_{10}(OH)_2$) obtained from the intensities of the elements in AEM-TEM analyses of samples A14 and B6

	A14(1)	A14(2)	B6
Si	3.93	3.89	3.95
Al IV	0.07	0.11	0.05
Al VI	1.42	0.92	1.03
Fe*	0.33	0.31	0.17
Mg	0.31	1.03	0.79
Ca	0.06	0.03	0.29
K	0.08	0.23	0.29
∑oct	2.06	2.26	1.99
∑inter	0.20	0.28	0.58

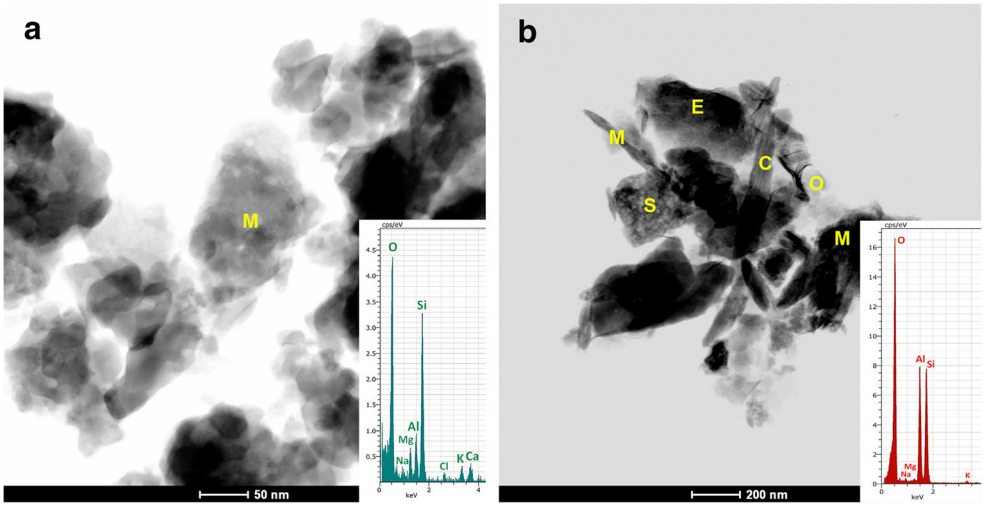

Fig. 8 **a** STEM image of a montmorillonite (M) type smectite particle from sample B6. **b** TEM image of sample A14 showing a varied group of particles with different compositions: montmorillonite (M), kaolinite (C), silica (S), Mn and Pb oxides (O), smectite (E). The inset graphs contain the EDX spectra for montmorillonite (**a**) and kaolinite (**b**)

gy. On the basis of the EDX spectra and the diffraction of electrons in a selected area (SAED), we identified amorphous phases of silica (Fig. 9a) with a lumpy or granular appearance, corresponding to the initial phases of alteration of volcanic glass. Other particles, which also had a granular porous appearance, could be attributed to crystalline aggregates of tridymite, as can be deduced from the EDX spectrum and from the spacings calculated on the basis of the diffraction rings in the SAED photograph (Fig. 9b).

As happened with the other techniques, in TEM, we searched for the possible presence of amorphous/nanocrystalline phases of calcium silicate hydrates (CSH) but were unable to find any.

Mercury intrusion porosimetry

The microscopy observations regarding the porosity were confirmed and completed using MIP. The samples we studied do indeed differ in terms of the accessible porosity values and the pore size distribution. In particular, A14 (mud brick) and B6 (rendering mortar) show a unimodal distribution, which is more pronounced in B6 with a maximum peak of pores at around 0.5 μm (Fig. 10). The other two samples, A27 (rendering mortar made from raw earth) and A32 (paving), showed a polymodal pore size distribution in which a more abundant family of pores could be identified between 0.3 and 0.5 μm, although this was not as pronounced as in the two previous samples, and other

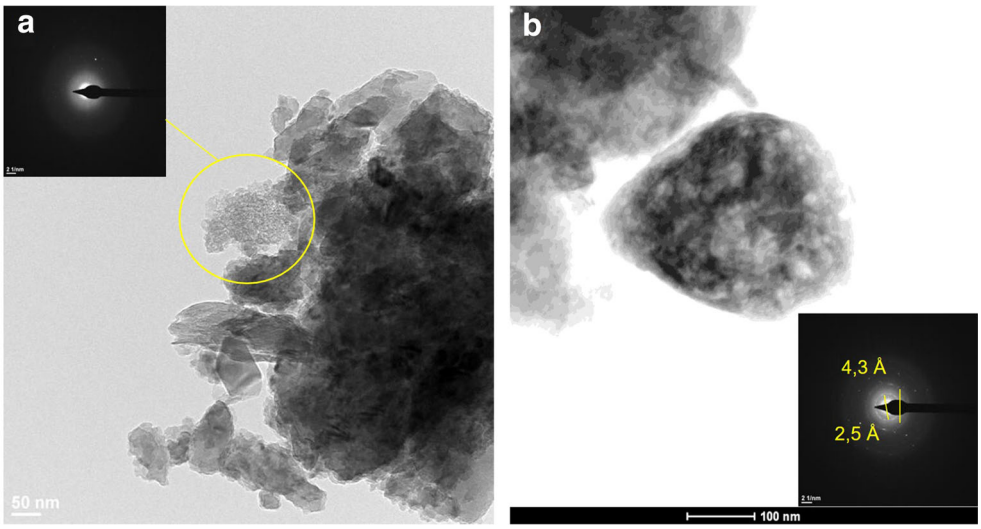

Fig. 9 **a** TEM image of sample A14 in which a particle of amorphous silica can be observed together with its corresponding electron diffraction pattern. **b** STEM image of sample A14 in which a particle of tridymite can be observed together with its corresponding diffraction and spacings

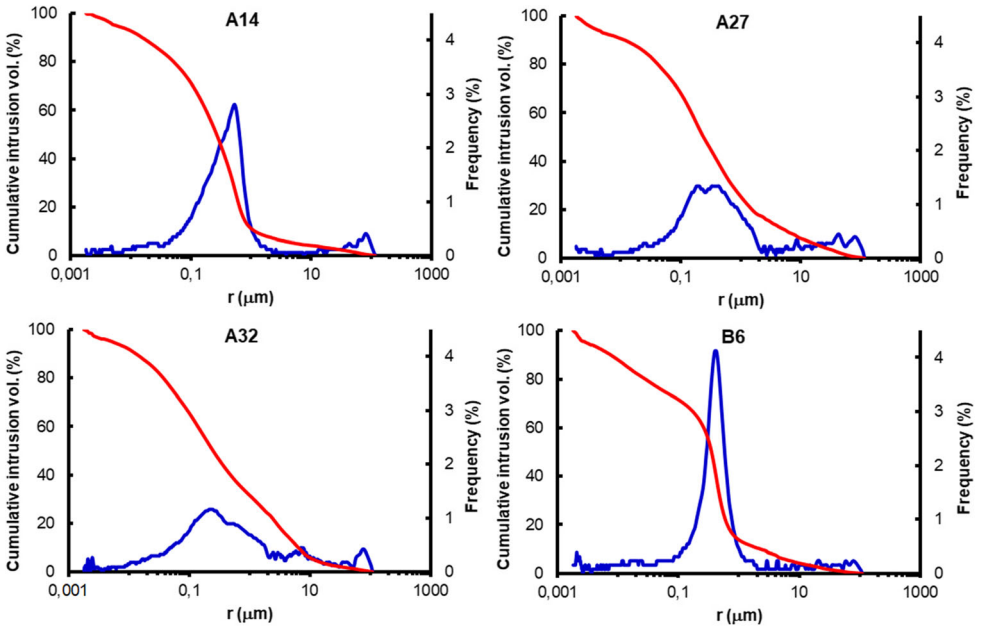

Fig. 10 Cumulative mercury intrusion porosity (red) and pore size distribution (blue) curves for selected archaeological samples

secondary groups at around 10 μm and 80 μm (Fig. 10). It is interesting to observe that porosity (P_o) increases as the pore size curve becomes less pointed (shifting from unimodal to polymodal), to such an extent that the porosity value for A32 is almost double that for B6 (~ 47% and ~ 25%, respectively, Table 4). The abundance of smaller pores has caused an increase in the specific surface area (SSA, Table 4), as can be seen in A32. As regards the density values, those for real density (ρ_r, Table 4) are dependent on the mineralogy of the samples. The values are similar to each other and in line with the density values for the silicates and carbonates identified by XRD. The apparent density (ρ_a, Table 4) depends on the presence of empty spaces in the samples. Indeed, the higher the P_o value, the greater the difference between ρ_a and ρ_r.

Table 4 Results of MIP analysis on selected archaeological samples. *SSA*, specific surface area (m^2/g); ρ_a, apparent density (g/cm^3); ρ_r, real density (g/cm^3); P_o, open porosity (%)

	A14	A27	A32	B6
SSA	9.5	13.46	21.79	11.23
ρ_a	1.79	1.79	1.38	1.92
ρ_r	2.6	2.63	2.59	2.55
P_o	31.19	32.08	46.56	24.73

Discussion of the analytical results

In the different constructions erected at the successive settlements at Niğde-Kınık Höyük, two basic groups of materials were used and reused. Firstly, huge numbers of large blocks were used in the defensive walls and in the walls for the dwellings, and secondly, fine grain materials were used to make mud bricks, renders, paving, etc. The blocks were hewn from different kinds of volcanic rocks from colluvial deposits from nearby volcanoes about 10 km away. Materials from these volcanoes can be found in the near vicinity of the settlement (Altın et al. 2015).

The results of our experiments show that the materials used to construct the Niğde-Kınık Höyük archaeological site are composed of raw (i.e., not artificially manufactured) fine grain volcanic sands proceeding from the materials found in the area, with the exception of the renders made of hardened mortar and those with a lime-based surface finish. The mineralogy is a typical result of the geological processes that take place in volcanic areas. We found quartz, cristobalite, tridymite, feldspars *s.l.*, mica, pyroxene, amphibole, olivine, and abundant fragments of volcanic glass, as well as other materials of sedimentary origin such as calcite, gypsum, and halite, possibly from lacustrine sediments from a paleolake (Altın et al. 2015). Clayey minerals were also found in very small amounts produced by the geological alteration of volcanic glass.

In spite of the fact that calcite is present in most of the diffractograms, when the samples were studied under POM and SEM, no calcite grains were detected. Calcite was observed above all as part of the matrix with a very fine grain size and forming rims around other grains or in the form of microcrystalline aggregates.

The XRD results show substantial amounts of cristobalite in most of the samples together with smaller quantities of tridymite, both of low temperature. These phases were not distinguishable in POM or in SEM due to their small size, but they were detected using TEM, which may indicate that they were part of the matrix. These minerals are produced by the natural alteration of acidic volcanic glass, which is unstable in nature and tends to evolve towards more stable phases. The first phase of alteration of volcanic glass is Opal-A (amorphous), which was probably identified in the particles of amorphous silica observed by diffraction in TEM. Later, the first crystalline phases begin to form, giving rise to the cristobalite and the tridymite that together form Opal-CT. However, it is also important to point out that the occasional, practically monomineralic, macroscopic grain of volcanic tridymite was detected with XRD.

Using TEM, it was possible to identify and characterize the minerals in the clay, which had not been detected with other techniques, very possibly because they were only found in very small amounts in the finest fraction. In particular, we identified smectites, kaolinite, and illite. Most of the smectites turned out to be montmorillonites, the most common type of dioctahedral smectite, with Mg-Fe, typical of the alteration of ferromagnesian minerals. Its most frequent origin is volcanic glass (Chamley 1989), which is quite abundant in the samples. The montmorillonite, cristobalite, tridymite, and amorphous silica also represent the first phases of alteration of the glass.

In this paper, special attention has been paid to the possible presence of calcium silicate hydrates (CSH) due to the fact that they play an important role in the preservation of ancient building materials (Hodgkinson and Hughes 1999), as has been observed in the case of Roman constructions with pozzolana (Moropoulou et al. 2005). Although we searched for these silicates with different analytical techniques, we were unable to find them. The presence of tobermorite, the crystalline phase of CSH, was not detected in the diffractograms. We also studied the relationships between Ca and Si in the spectrum performed using EDX compositional analysis in SEM and did not find any that might correspond to CSH phases. This would suggest that the high concentrations of calcium present in some spectra may be due to contamination from calcite particles from the matrix. Lastly, using TEM, we identified various amorphous silica phases (Fig. 9a), but did not obtain any compositions or textures typical of CSH (Elert et al. 2017, 2018).

Conclusions

Two kinds of building materials were used in the construction of Niğde-Kınık Höyük. Both were of volcanic origin and were obtained near the site. These were, firstly, large blocks of stone and, secondly, fine-grained building materials used for making mud bricks, renders, and paving. This second group of materials were made up of fine-grained volcanic sands with a fundamentally volcanic (quartz, feldspars *s.l.*, cristobalite, pyroxenes, micas, amphiboles, and olivine) and sedimentary (calcite) mineralogy, together with small amounts of clayey minerals.

These building materials seem to have been used as found in nature, without any additional materials or artificial manufacturing processes (e.g., firing) that might alter their properties, with the exception of some of the renders and paving materials which either have a lime finish or are made of a more compact, hardened lime mortar.

In view of these results, it could be argued that there is no intrinsic characteristic of these materials or of the process of preparation or of application in the building itself which would justify the excellent state of conservation of the Niğde-Kınık Höyük. In fact, as has been mentioned in the earlier sections, the materials are not particularly compact, and after being uncovered in recent excavations, they started to deteriorate more quickly. This leads us to conclude that they may have been conserved for such a long time due to the fact that they were buried under constant temperature and humidity conditions and were protected from the direct action of agents such as rain, snow, and wind.

Acknowledgements We are grateful to Nigel Walkington for his assistance in translating the original text. We are equally grateful to Prof. Ali Gurel who kindly assigned us the study of these samples. The work is the results of the collaboration between the authors. For the sake of the evaluation of the research in the Humanities in Italy, L. d'Alfonso is responsible for the part entitled: Archaeological and construction analysis.

Funding This study received financial support from Research Group RNM179 of the Junta de Andalucía and Research Project MAT2016-75889-R.

References

Altın T, El Ouahabi M, Fagel N (2015) Environmental and climatic changes during the Pleistocene–Holocene in the Bor Plain, Central Anatolia, Turkey. Palaeogeogr Palaeoclimatol Palaeoecol 440:564–578

Balatti S, Balza ME (2012) Kınık Höyük and Southern Cappadocia (Turkey): Geo-archaeological activities, landscapes and social spaces. In: Hofmann R, Moetz FK, Müller J (eds) Social and environmental space, vol 3. R. Habelt, Bonn, pp 93–104

Beyer D (2010) From the Bronze Age to the Iron Age at Zeyve Höyük/Porsuk: a temporary review. In: Geo-archaeological activities in Southern Cappadocia – Turkey, edited by Lorenzo d'Alfonso, Maria Elena Balza, and Clelia Mora, 97–109. Studia Mediterranea 22. Italian University Press, Pavia

Beyer D (2015) Quelques nouvelles données sur la chronologie des phases anciennes de Porsuk, du Bronze Moyen à la réoccupation du Fer. In: Beyer D, Henry O, Tibet A (eds) La Cappadoce méridionale: de la préhistoire à la période byzantine. Institut Français d'Etudes Anatoliennes Georges-Dumézil, Istanbul, pp 101–110

Cerny R, Kunca A, Tydlitát V, Drchalová J, Rovnaníková P (2006) Effect of pozzolanic admixtures on mechanical, thermal and hygric properties of lime plasters. Constr Build Mater 20:849–857

Chamley H (1989) Clay sedimentology. Springer, Berlin, 623 pp

Cinieri V, d'Alfonso L, Morandotti M (2014) Building techniques of fortified structures in Kınık Höyük archaeological excavation (Turkey). In: Peña F, Chávez M (eds) 9th International Conference on Structural Analysis of Historical Constructions, pp 1–14

Cinieri V, Morandotti M, Setti M, Zamperini E (2016) Analisi e conservazione del patrimonio archeologico di Kınık Höyük. In: REUSO Congress, Pavia (Italy), pp 392–399

Cizer O (2009) Competition between carbonation and hydration on the hardening of calcium hydroxide and calcium silicate binders. PhD Thesis, Katholieke Universiteit Leuven, Belgium.

d'Alfonso L (2010) Geo-archaeological survey in northern Tyanitis and the ancient history of Southern Cappadocia. In: Geo-archaeological activities in Southern Cappadocia (Turkey). Proceedings of the Meeting held at Pavia, 20.11.2008, (d'Alfonso, Balza, Mora, eds), vol 22, pp 27–52

d'Alfonso L, Castellano L (2018) Kınık Hoyük in south Cappadocia. Addendum to: A Comparative stratigraphy of Cilicia. Altorientalische Forschungen 45(1):84–93

d'Alfonso L, Mora C (2007) "Viaggi anatolici" dell'Università di Pavia. Rapporto preliminare della prima campagna di ricognizione archeologica nella Tyanitide settentrionale. Athenaeum, 95, 819-836.

d'Alfonso L, Mora C (2010) Missione archeologica in Cappadocia meridionale: 2010. Atenhaeum 90(2):549–564

d'Alfonso L, Mora C (2012) Il progetto di Kınık Höyük. Missione archeologica e ricerche storiche in Cappadocia meridionale (Turchia). Atenhaeum 100:529–538

d'Alfonso L, Gorrini ME, Mora C (2014) Archaeological excavations at Kınık Höyük. Preliminary report of the third campaign (2013). Athenaeum 102:565–586

d'Alfonso L, Yolaçan B, Castellano L, Highcock N, Casagrande-Kim R, Gorrini ME, Trameri A (2020) Niğde Kınık Höyük: new evidence on Central Anatolia during the first millennium BCE. Near Eastern Archaeology 83:1,16–1,29

Deniel C, Aydar E, Gourgaud A (1998) The Hasan Dagi stratovolcano (central Anatolia, Turkey): evolution from calc-alkaline to alkaline magmatism in a collision zone. J Volcanol Geotherm Res 87:275–302

Dhont D, Chorowicz J, Yürür T, Froger JL, Köse O, Gündoğdu NM (1998) Emplacement of volcanic vents and geodynamics of Central Anatolia Turkey. J Volcanol Geotherm Res 85:33–54

Elert K, Nieto F, Azañón JM (2017) Effects of lime treatments on marls. Appl. Clay Sci 135:611–619

Elert K, Nieto F, Azañón JM (2018) Smectite formation upon lime stabilization of expansive marls. Appl. Clay Sci 158:29–36

Gürel A, Lermi A (2010) Pleistocene-Holocene fills of the Ereğli-Bor Plain (Central Anatolia): recent geo-archaeological contributions. In: Geo-archaeological activities in Southern Cappadocia, Turkey, (L. d'Alfonso, M.E. Balza & C. Mora, eds). Studia Mediterranea 22: 55–68

Highcock NE, Crabtree P, Campana D, Capardoni M, Lanaro A, Matessi A, Miller NF, Stroshal P, Trameri A, d'Alfonso L (2015) Kınık Höyük, Niğde: a new archaeological project in Southern Cappadocia. In: Steadman SR, McMahon G (eds) The archaeology of Anatolia: recent discoveries (2011-2014). Cambridge Scholars Publishing, New Castle, pp 98–127

Hodgkinson ES, Hughes CR (1999) The mineralogy and geochemistry of cement/rock reactions: high-resolution studies of experimental and analogue materials. In: Metcalfe R, Rochelle CA (eds) Chemical containment of waste in the geosphere. Geol. Soc. London Spec. Pub. 157. The Geological Society of London, pp 195–211

Innocenti F, Mazzuoli R, Pasquaré G, Redicati de Brozolo F, Villari L (1975) The Neogene calk-alkaline volcanism of central Anatolia: geochronological data from the Kayseri-Nigde area. Geol Mag 112:349–360

Innocenti F, Manetti P, Mazzuoli R, Pasquaré G, Villari L (1982a) Anatolia and Northern Iran. In: Thorpe RS (ed) Andesites, orogenic andesites and related rocks. The Open. John Wiley & Sons, Chichester, pp 327–349

Innocenti F, Mazzuoli R, Pasquaré G, Radicati di Brozolo F, Villari L (1982b) Tertiary and Quaternary volcanism of the Erzurum-Kars area (Eastern Turkey): geochronological data and geodynamic evolution. J Volcanol Geotherm Res 13:223–240

Kurkcuoglu B, Sen E, Aydar E, Gourgaud A, Gundogdu N (1988) Geochemical approach to magmatic evolution of Mt. Erciyes stratovolcano, central Anatolia, Turkey. J Volcanol Geotherm Res 85: 473–494

Kuşcu G, Geneli F (2010) Review of post-collisional volcanism in the Central Anatolian Volcanic Province (Turkey), with special reference to the Tepekoy Volcanic Complex. Int J Earth Sci 99:593–621

Larsen MT (2015) Ancient Kanesh: a merchant colony in Bronze Age Anatolia. Cambridge University Press, New York, NY. https://doi.org/10.1017/CBO9781316344781

Lorimer GW, Cliff G (1976) Analytical electron microscopy of minerals. In: H.-R. Wenk, Electron Microscopy in Mineralogy. Springer, pp 506–519

Matessi A, Capardoni M, Lanaro A (2014) Excavations at Kınık Höyük: a preliminary report on the first campaign (Aug. - Oct. 2011). In: Bieliński P, Gawlikowski M, Koliński R, Ławecka D, Sołtysiak A, Wygnańska Z (eds) Proceedings of the 8th International Congress on the Archaeology of the Ancient Near East, Volume 2: Excavations and Progress Report Posters, Wiesbaden, pp 321–340

MGM (Turkish State Meteorological Service) (2019) https://mgm.gov.tr/eng/forecast-cities.aspx?m=NIGDE#.Mapy.cz : https://en.mapy.cz/zakladni?x=35.5705462&y=37.5200564&z=6

Moropoulou A, Bakolas A, Anagnostopoulou S (2005) Composite materials in ancient structures. Cem Concr Compos 27:295–300

Özgüç T (2005) Kültepe: Kaniš/Neša. 1. baskı. Yapı Kredi Yayınları (Series) 2210. Yapı Kredi Yayınları, İstanbul

Pasquaré G, Poli S, Venzolli L, Zanchi A (1988) Continental arc volcanism and tectonic setting in Central Anatolia. Tectonophysics 146: 217–230

Piper JDA, Koçbulut F, Gürsoy H, Tatar O, Viereck L, Lepetit P, Roberts AP, Akpınar Z (2013) Palaeomagnetism of the Cappadocian Volcanic Succession, Central Turkey: major ignimbrite emplacement during two short (Miocene) episodes and Neogene tectonics of the Anatolian collage. J Volcanol Geotherm Res 262:47–67

Smith D (1998) Opal, cristobalite, and tridymite: noncrystallinity versus crystallinity, nomenclature of the silica minerals and bibliography. Powder Diffract 13(1):2–19. https://doi.org/10.1017/S0885715600009696

Theodoridou M, Ioannou I, Philokyprou M (2013) New evidence of early use of artificial pozzolanic material in mortars. J Archaeol Sci 40: 3263–3269

Toprak V (1994) Volcano-tectonic features of the Cappadocian volcanic province. International Volcanological Congress Excursion Guide, Ankara, 58 p